

# Journal of Materials Chemistry A

Accepted Manuscript

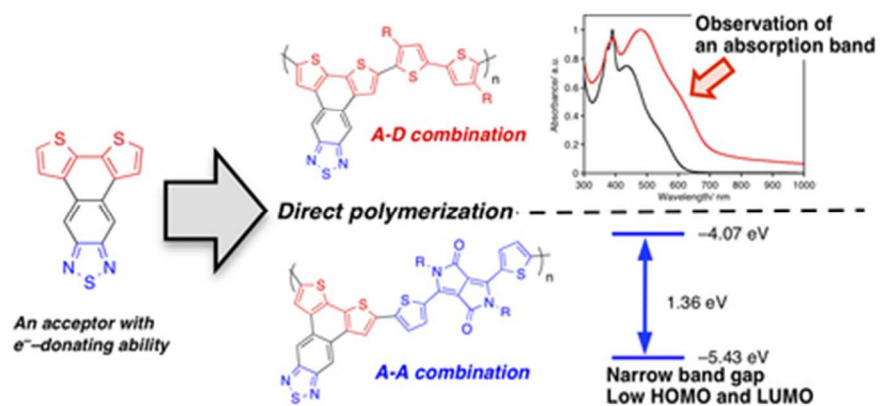


This is an *Accepted Manuscript*, which has been through the Royal Society of Chemistry peer review process and has been accepted for publication.

*Accepted Manuscripts* are published online shortly after acceptance, before technical editing, formatting and proof reading. Using this free service, authors can make their results available to the community, in citable form, before we publish the edited article. We will replace this *Accepted Manuscript* with the edited and formatted *Advance Article* as soon as it is available.

You can find more information about *Accepted Manuscripts* in the [Information for Authors](#).

Please note that technical editing may introduce minor changes to the text and/or graphics, which may alter content. The journal's standard [Terms & Conditions](#) and the [Ethical guidelines](#) still apply. In no event shall the Royal Society of Chemistry be held responsible for any errors or omissions in this *Accepted Manuscript* or any consequences arising from the use of any information it contains.



37x17mm (300 x 300 DPI)

Cite this: DOI: 10.1039/c0xx00000x

www.rsc.org/xxxxxx

ARTICLE TYPE

# Synthesis and optical properties of photovoltaic materials based on the ambipolar unit dithienonaphthothiadiazole

Tatsuaki Nakanishi,<sup>a</sup> Yasuhiro Shirai<sup>\*a,b</sup> and Liyuan Han<sup>\*b,c</sup>

Received (in XXX, XXX) Xth XXXXXXXXX 20XX, Accepted Xth XXXXXXXXX 20XX

DOI: 10.1039/b000000x

Dithieno[3'2':5,6;2'',3'':7,8]naphtho[2,3-c][1,2,5]thiadiazole (DTNT) was designed to control the band energies of the polymers for photovoltaic materials. Electrochemical analysis showed that DTNT acts as both an electron donor and an electron acceptor, revealing the ambipolar nature of the DTNT unit. The direct arylation polymerization of DTNT with 2,2'-bithiophene (BTh) and 3,6-bis(2-thienyl)pyrrolo[3,4-c]pyrrole-1,4-dione (DPP) afforded four polymers that differed in either the unit of copolymerization or the chosen side chains. In the **PDTNT-BTh** series, a shoulder absorption band was observed at a longer wavelength than the intense absorption band. The **PDTNT-DPP** series exhibited a narrow band gap of less than 1.4 eV and a low HOMO energy of  $-5.43$  eV. An organic photovoltaic cell that contained a **PDTNT-BTh** polymer with 2-ethylhexyl groups and [6,6]-phenyl C<sub>71</sub> butyric acid methyl ester (PC<sub>71</sub>BM) as an active layer afforded the best performance among the studied compounds, with a  $J_{SC}$  of  $6.98$  mA/cm<sup>2</sup>, a  $V_{OC}$  of  $0.758$  V, a  $FF$  of  $0.52$ , and a PCE of  $2.76\%$ .

## 15 Introduction

Organic photovoltaics (OPVs) have attracted significant attention as they are a complementary of silicon solar cells, rather than being an alternative, with characteristic lightness, flexibility, transparency, and potential for fabrication of large-area modules at low cost.<sup>1,2</sup> In the past decade, enormous efforts have been devoted to achieving power conversion efficiencies (PCEs) of OPVs up to over  $10\%$ .<sup>3</sup> However, to improve the PCE of OPV devices, numerous issues still need to be addressed, such as effective light harvesting,<sup>4</sup> energy level control of the highest occupied molecular orbital (HOMO) of polymers and the lowest unoccupied molecular orbital (LUMO) of fullerene derivatives,<sup>5</sup> increased solubility and miscibility of the materials by introducing solubilizing groups to attain the best bulk heterojunction structure,<sup>6</sup> the use of additives to control the crystallinity of the materials during solvent evaporation,<sup>7</sup> and the blending of other dyes to aid light collection.<sup>8</sup> With respect to the general design of the polymer scaffold, the light absorption and HOMO and LUMO levels of the polymers can be modulated by a combination of the component monomer units.

35 There are two main approaches to develop narrow band gap polymers for OPV cells, which are able to collect more sunlight of strong intensity ranging from the visible to the near-infrared region to improve a short-circuit current density ( $J_{SC}$ ). The first

incorporation of fused ring systems like benzo[*c*]thiophene, thieno[3,4-*b*]pyrazine, thieno[3,4-*b*]thiophene and a variety of other related systems.<sup>9-11</sup> The second approach involves the use of a donor-acceptor (D-A) polymer, in which an electron rich donor and an electron deficient acceptor are covalently linked alternatively to form a long polymer chain. In general, given the proper structures and energy levels for the donor and the acceptor parts, this approach results in intramolecular charge-transfer (ICT) and a lowering of the band gap.<sup>12,13</sup>

50 A system with broad absorption is also important to collect light and provide a high  $J_{SC}$  value. Reynolds and coworkers presented models for the case of dual-band absorption in D-A polymers.<sup>14</sup> In their proposed models for D-A polymers, the absorption with the longest wavelength originates from an ICT transition between a donor and an acceptor, and the absorption with second longest wavelength originates from a  $\pi$ - $\pi^*$  transition in a continuous array of donors or acceptors in a repeat unit. The intensity of these two absorption bands can be controlled by varying the concentrations of electron-rich and electron-deficient components along the polymer backbone. In other words, the dual absorption can be tuned by altering the number of linking units between a donor and an acceptor.

The introduction of  $\pi$ -chromophores into conjugated polymers through a double bond is another way to harvest more sunlight.<sup>15</sup> In a uniform, alternative, or random backbone, a pendant donor acts as an independent pigment to absorb sunlight in the shorter-wavelength region, and a pendant acceptor can exhibit an ICT band to collect sunlight at longer wavelength.

A decrease in the HOMO energy of a polymer leads to an improvement of an open-circuit voltage ( $V_{OC}$ ). As the strength of electron donating ability of a donor moiety affects the HOMO energy of the polymer, weak donors were first used as components in photovoltaic copolymers. Subsequently, many researchers tried to introduce electron-withdrawing groups into electron acceptors, e.g., groups such as fluoro,<sup>16</sup> cyano,<sup>17</sup> ester,<sup>18</sup> and added nitrogen to the electron deficient scaffold in the conventional linker and acceptors (e.g., thiazole, thiazolothiazole, pyridinothiadiazole etc.)<sup>19</sup> to decrease the HOMO energy of D-A polymers.

80 As a part of our program aimed at developing polymers that

<sup>a</sup> Global Research center for Environment and Energy based on Nanomaterials Science (GREEN), National Institute for Materials Science (NIMS), 1-1 Namiki, Tsukuba, Ibaraki, 305-0044. Tel: +81-29-860-4792; E-mail: SHIRAI.Yasuhiro@nims.go.jp

<sup>b</sup> Photovoltaic Materials Unit, National Institute for Materials Science (MINS), 1-2-1 Sengen, Tsukuba, 305-0047 Japan. Tel: +81-29-859-2305; E-mail: HAN.Liyuan@nims.go.jp

<sup>c</sup> Core Research for Evolutional Science and Technology (CREST), Japan Science and Technology Agency (JST), 7 Gobancho, Chiyoda-ku, Tokyo, 102-0076 Japan.

approach to lowering the band gap is to enhance the quinoid character of the backbone, which can be accomplished via the

satisfy the requirements outlined above for light absorption and HOMO and LUMO energies, we designed a T-shaped monomer, dithieno[3',2':5,6;2'',3'':7,8]naphtho[2,3-c][1,2,5]thiadiazole (DTNT) as shown in Figure 1. The thiophene parts are electron-donating units and these also act as linkers to another unit due to the high reactivity at the  $\alpha$  positions. The thiadiazole unit acts as an electron acceptor to decrease the HOMO energy of the system. With a proper combination of the electron donor and acceptor part in the DTNT, it can possibly exhibit unique donor and/or acceptor properties. Such dual donor and acceptor behaviour in related systems has been recently reported by Rasmussen, who has proposed the term "ambipolar" to describe this simultaneous donor and acceptor nature.<sup>20</sup> The fused naphthalene ring plays an important role in extending the  $\pi$  system of the molecule, in a manner similar to the acene series, to cause a bathochromic shift in the absorption maximum of the molecule. For example, the longest absorption maxima for the acene series are markedly red-shifted on increasing the number of phenyl rings (anthracene, 380 nm;<sup>21</sup> tetracene, 470 nm;<sup>22</sup> pentacene, 670 nm<sup>23</sup>).

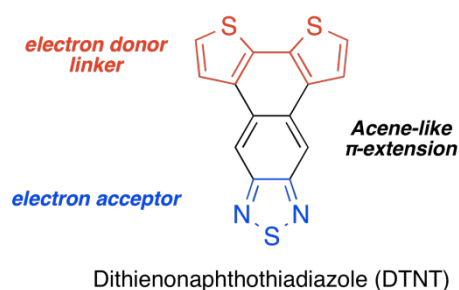


**Figure 1.** Design concept for DTNT

This study describes the synthesis of the novel ambipolar DTNT unit with two aims in mind: (i) to broaden the range of the absorption wavelength and (ii) to obtain a narrow band gap with a low HOMO energy. Four polymers (Figure 2) were prepared by direct arylation polymerization<sup>24,25</sup> due to the low solubility of DTNT in common solvents. Since DTNT contains both donor and acceptor moieties, the counterparts that have different electronic character are employed, namely 2,2'-bithiophene (BTh) and 3,6-bis(2-thienyl)pyrrolo[3,4-c]pyrrole-1,4-dione (DPP). The optical, electrochemical, and solubility properties were characterized and the OPV applications of three polymers were evaluated under AM1.5G conditions. It was successfully demonstrated that the combination of DTNT and the electron-donating BTh group enables the absorption range to be broadened by creating an absorption band in longer-wavelength region. It was found that the combination of DTNT, which has a weak electron-accepting ability, and a strong electron acceptor (DPP) provides a narrow band gap polymer with low HOMO and LUMO energies.

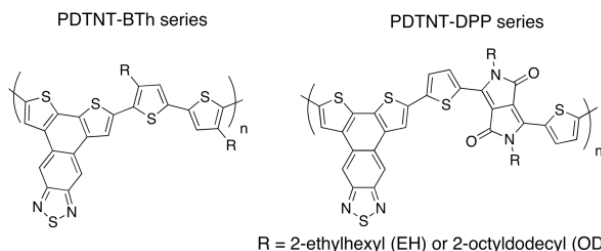
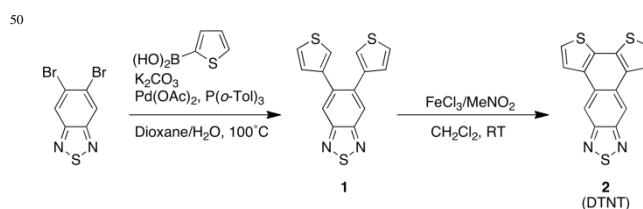


**Figure 2.** Chemical structures of the PDTNT-BTh series and PDTNT-DPP series

## Results and discussion

### Synthesis and physical properties of DTNT

The Suzuki coupling of 4,5-dibromobenzothiadiazole with 3-thiopheneboronic acid followed by oxidative cyclization using  $\text{FeCl}_3$  afforded DTNT as a red powder (Scheme 1). It was difficult to prepare a fine thin film of DTNT by either thermal deposition or spin-coating due to island formations.



**Scheme 1.** Synthetic route for dithienonaphthothiadiazole (DTNT, 2).

The absorption spectrum of DTNT in *o*-dichlorobenzene (*o*DCB) is shown in Figure 3. In solution, for DTNT, two absorption maxima in the region at 368 and 386 nm and one weak broad absorption band in the visible region at 449 nm were observed with an onset wavelength of 506 nm (= 2.45 eV).

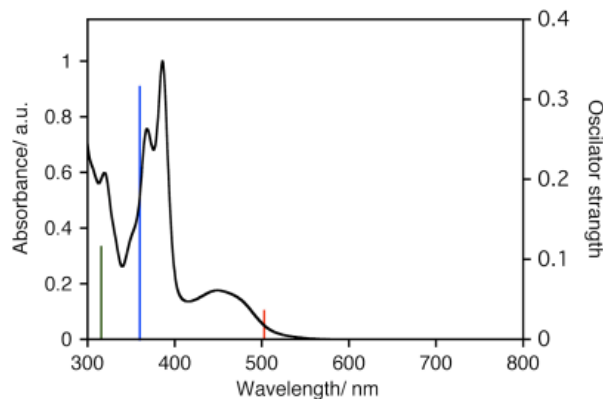


**Figure 3.** Absorption spectra of DTNT in *o*DCB. Bars indicate the oscillator strength of DTNT calculated by TD-DFT at the B3LYP/6-311G(d,p) level of theory.

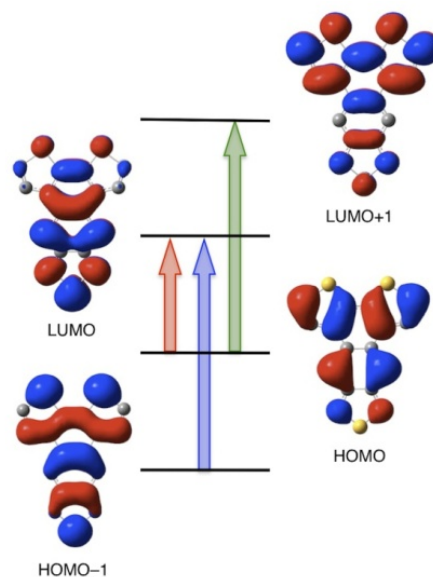


**Figure 4.** Frontier orbitals of DTNT. The arrows show the assignment of transitions for each absorption band in the bar graph in Figure 3.

The absorption bands were assigned by carrying out a TD-DFT calculation at the B3LYP hybrid functional with the 6-311G(d,p) basis set. Geometry optimization and vibrational frequency analysis were conducted at the B3LYP/6-31G(d) level of theory. The frontier orbitals of DTNT are shown in Figure 4. Three absorption bands were calculated for the absorption of DTNT, as shown in the bar graph in Figure 3. The longest wavelength absorption band at 449 nm corresponded to the transition from the HOMO to the LUMO. The second longest wavelength band at 368–386 nm could be assigned to the transition from the HOMO–1 to the LUMO, and the other band at 320 nm was assigned to that from the HOMO to the LUMO+1. The energy difference between the absorption maxima at 368 and 386 nm was 0.157 eV ( $= 1267 \text{ cm}^{-1}$ ); hence, the absorption maximum at 368 nm is considered to be due to the transition to a higher vibration level than that at 386 nm. The HOMO–1 and the LUMO+1 were delocalized over the molecule, whereas the HOMO was primarily localized on the dithienonaphthalene moiety of DTNT, and the LUMO disproportionately localized to the naphthothiadiazole moiety.

The cyclic voltammogram of DTNT in dichloromethane (DCM) containing 0.1 M of tetrabutylammonium hexafluorophosphate (TBAPF<sub>6</sub>) as a supporting electrolyte under argon is shown in Figure 5. One reversible redox wave was observed at  $E_{1/2}^{\text{red}} = -1.72 \text{ V}$  (vs Fc/Fc<sup>+</sup>) with an onset potential of  $-1.60 \text{ V}$ . DTNT exhibited an irreversible oxidation at 1.08 eV, probably due to the electrochemical condensation reactions of DTNT. The onset potential was 0.78 V. Thus, DTNT can act as both an electron donor and electron acceptor. Electrochemical HOMO and LUMO energies ( $E_{\text{HOMO}}^{\text{ec}}$  and  $E_{\text{LUMO}}^{\text{ec}}$ ) were estimated from the onset of the oxidation and reduction peaks to be  $-5.88 \text{ eV}$  and  $-3.50 \text{ eV}$ , respectively, according to equations 1 and 2.<sup>26</sup>

$$E_{\text{HOMO}}^{\text{ec}} = -e(E_{\text{ox}}^{\text{onset}} \text{ (vs Fc/Fc}^+) + 5.1) \quad (1)$$

$$E_{\text{LUMO}}^{\text{ec}} = -e(E_{\text{red}}^{\text{onset}} \text{ (vs Fc/Fc}^+) + 5.1) \quad (2)$$

Here  $E_{\text{ox}}^{\text{onset}}$  and  $E_{\text{red}}^{\text{onset}}$  represent the onset potentials of oxidation and reduction. The energy of the HOMO of a drop-cast film of DTNT was also estimated to be  $-6.06 \text{ eV}$  using photoelectron spectroscopy in air (PESA) on an AC-3 spectrometer (RIKEN KEIKI Co., Ltd.). The LUMO energy estimated using the work function ( $-6.06 \text{ eV}$ ) and the optical gap energy ( $2.45 \text{ eV}$ ) was  $-3.61 \text{ eV}$ .

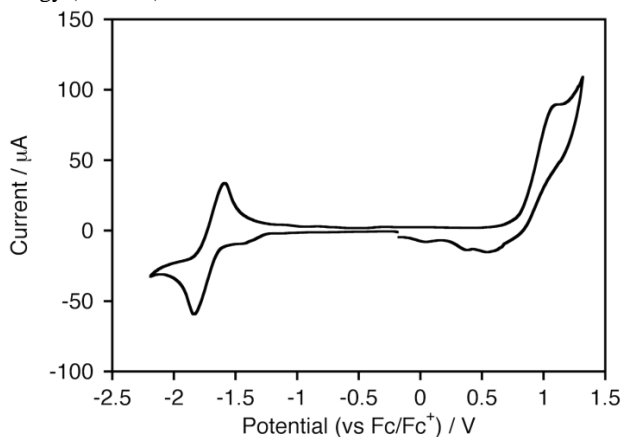
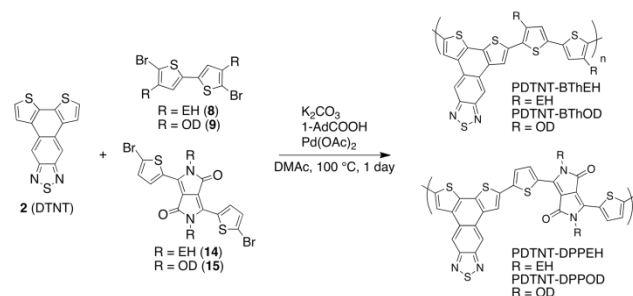


**Figure 5.** Cyclic voltammogram of 3.1 mM of DTNT in DCM.

### Polymer synthesis

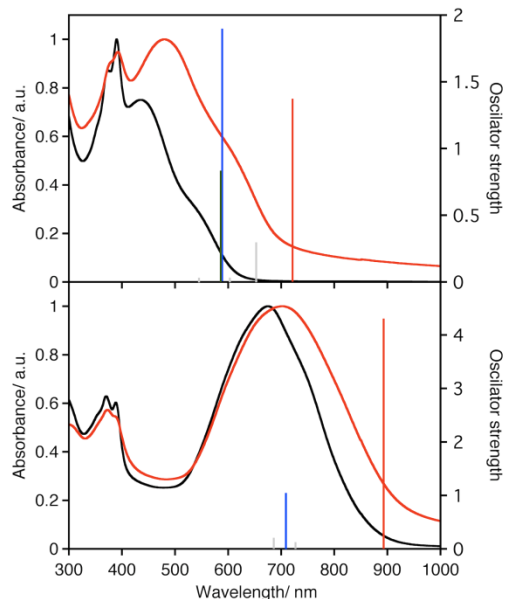
Generally, conjugated copolymers are prepared via Suzuki or Stille coupling with a dibrominated precursor and a diborylated or distannylated one. The latter is synthesized by lithiation followed by metallation. In the case of DTNT, no lithiation took place in THF at RT, probably due to the limited solubility. The bromination of DTNT even in H<sub>2</sub>SO<sub>4</sub> with NBS proceeded only up to monobromination. Fortunately, we found later that the electrochemical polymerization of the unsubstituted DTNT can take place, we therefore tried direct arylation using this unsubstituted DTNT for polymer preparations. Electrochemical measurement showed that DTNT acts as both an electron donor and an electron acceptor; hence, we employed an electron donor and an electron acceptor as counterparts, BTh and DPP units with 2-ethylhexyl (EH) and 2-octyldodecyl (OD) groups as solubilizing groups in appropriate positions. Direct polymerization was conducted with potassium carbonate, 1-adamantane carboxylic acid, and palladium acetate in *N,N*-dimethylacetamide (DMAc), as modified by Kanbara and coworkers.<sup>25</sup> Finally, four DTNT-based polymers were afforded: **PDTNT-BTheH**, **PDTNT-BThOD**, **PDTNT-DPPEH**, and **PDTNT-DPPOD** (Scheme 2). Details for the synthesis of the precursors are provided in the Supporting Information. After polymerization, the reaction mixtures were poured into methanol and the precipitates were filtrated using a membrane filter with a pore size of 0.45 µm. The resulting polymers had different solubilities; therefore, the purification method was different for each polymer. For **PDTNT-BTheH**, **PDTNT-DPPEH**, and **PDTNT-DPPOD**, successive Soxhlet extractions were performed with hexane, acetone, and chloroform (CF). In the case of **PDTNT-DPPEH**, a further extraction step with chlorobenzene (CB) was conducted, and the final fractions were collected. **PDTNT-BThOD** was soluble even in hexane, and purification was therefore performed successively with BioBeads<sup>®</sup>, first with an exclusion limit of 16000 and second with an exclusion limit of 2000 to remove the low molecular weight fraction. Number average molecular weights ( $M_n$ ), approximate degrees of polymerization ( $n$ ), and polydispersity indices (PDI) were determined by GPC with THF as eluent at 40 °C, and the results are summarized in Table 2 and Figure S4. The results indicate that the polymers synthesized by the direct arylation of the DTNT gave higher fractions of low molecular weight polymers, probably due to the low solubility and/or reactivity of the DTNT unit toward the direct arylation conditions used. We have repeated the direct arylation using microwave heating or other solvent such as *N*-methylpyrrolidone (NMP) that could increase the solubility, however, all attempts gave similar results with no improvement. Nevertheless, the GPC chromatograph (Figure S4) show small fractions (~5%) of higher molecular weight polymers over 10 kDa, and the characterization of energy levels for these materials will manifest the property of polymers containing the ambipolar DTNT unit.



**Scheme 2.** Synthesis of DTNT based polymers

**Table 2.** Molecular weights and polydispersity indices of the polymers

polymer	$M_n$ /kDa	$M_w$ /kDa	PDI	n
PDTNT-BTheH	5.1	6.0	1.17	~7
PDTNT-BThOD	5.2	6.2	1.19	~5
PDTNT-DPPEH	1.2	1.6	1.32	~2
PDTNT-DPPOD	5.5	9.1	1.66	~5

**Physical properties of polymers****Figure 6.** Absorption spectra of PDTNT-BThOD (top) in *o*DCB (black) or film (red), and PDTNT-DPPOD (bottom) in *o*DCB (black) or film (red). Bars in the graph are the calculated absorption bands.

The optical properties of the polymers were investigated by UV-Vis spectroscopy in *o*DCB solution and of thin films. The absorption spectra of PDTNT-BThOD and PDTNT-DPPOD are shown in Figure 6. The spectra of PDTNT-BTheH and PDTNT-DPPEH, which exhibited poor film formation properties, are shown in Figure S1 and S2. The optical data for the polymer films are summarized in Table 3. Three absorption bands were observed in both solution and thin film spectra of PDTNT-BThOD. In the films, the absorption band at around 380 nm was hardly shifted at all in comparison to that in solution, whereas the others were shifted from 530 and 436 nm (solution) to 590 and 481 nm (film), respectively.

**Table 3.** Absorption maxima and their extinction coefficients and band gap energies, the HOMO and the LUMO levels of the polymers

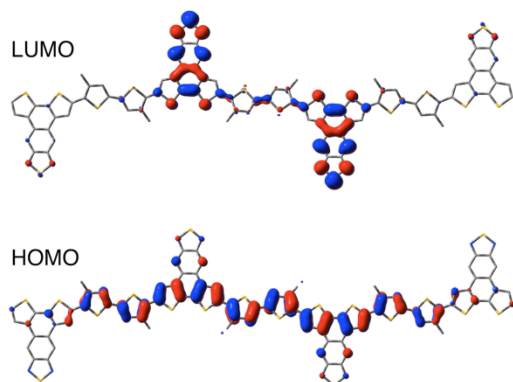
	In solution		Thin film		
	$\lambda_{\max}^a$ / nm	$\lambda_{\max}^b$ / nm	$E_{\text{gap}}^{\text{opt}c}$ / eV	$E_{\text{HOMO}}^{\text{opt}}$ / eV	$E_{\text{LUMO}}^{\text{opt}d}$ / eV
PDTNT-BTheH	374 (6.7), 390 (7.9), 435 (5.9), 525 (sh)	390, 481	1.80	-5.21	-3.41
PDTNT-BThOD	374 (28), 390 (32), 436 (24), 530 (sh)	378 (sh), 392, 481, 590 (sh)	1.79	-5.26	-3.47
PDTNT-DPPEH	371 (6.6), 388 (6.9), 675 (11)	374, 676	1.39	-5.46	-4.07
PDTNT-DPPOD	370 (26), 388 (25), 675 (42)	372, 392 (sh), 702	1.36	-5.43	-4.07

<sup>a</sup> Measured in *o*DCB, sh = shoulder, extinction coefficients in  $10^3 \text{ } \epsilon' \text{ M}^{-1} \text{ cm}^{-1}$  are listed in parentheses. <sup>b</sup> Measured in a film. <sup>c</sup> Calculated from the following equation:  $E_{\text{gap}}^{\text{opt}} = 1240/\lambda_{\text{onset}}$ . <sup>d</sup>  $E_{\text{LUMO}}^{\text{opt}} = E_{\text{HOMO}}^{\text{opt}} - E_{\text{gap}}^{\text{opt}}$ .

The band at around 380 nm was similar in shape and position to that due to the original  $\pi$ - $\pi^*$  transition of the DTNT monomer. In the films, the intensity of the second lowest energy absorption band was greater than that of the absorption band at around 380 nm. PDTNT-DPPOD exhibited two absorption bands in both solution and film samples. Only a very slight shift was observed in the band at around 380 nm on comparing the film and solution spectra, while the lowest energy absorption band at 675 nm was red-shifted to 702 nm in the film spectrum. The intensity ratio of the first and second bands was virtually identical in both solution and film spectra. It is noteworthy that all of the polymers investigated here retained the intense  $\pi$ - $\pi^*$  transition of the original DTNT at around 380 nm. The absorption onsets were 690 nm (=1.80 eV) for PDTNT-BTheH, 694 nm (=1.79 eV) for PDTNT-BThOD, 891 nm (=1.39 eV) for PDTNT-DPPEH, and 915 nm (=1.36 eV) for PDTNT-DPPOD, respectively. Electrochemical data for polymers were not obtained due to the difficulty in processing the polymers into film samples for electrochemical measurements. The HOMO energies of the polymer films were measured by PESA, and the band gaps of the polymers estimated from the onset of the absorption spectrum were used to determine the HOMO and LUMO energies. The values are -5.21 eV and -3.41 eV for PDTNT-BTheH, -5.26 eV and -3.47 eV for PDTNT-BThOD, -5.46 eV and -4.07 eV for PDTNT-DPPEH, and -5.43 eV and -4.07 eV for PDTNT-DPPOD. Despite the higher content of small molecular weight fractions for the PDTNT-DPPEH (Figure S4), it still exhibited similar HOMO and LUMO energies to that of PDTNT-DPPOD. The shape of the UV-visible spectra may be different from the polymers that have higher molecular weight because the extinction coefficients vary with the length of the polymer. Nevertheless, the HOMO and LUMO energy levels are sensitive to the high-molecular-weight polymer fractions, and the results indicate that small amount of high molecular weight polymers with enough number of repeating units to exhibit the saturation of the electronic and optical properties exist in all the polymer samples.

**Theoretical studies**

## (a) PDTNT-BTh series



## (b) PDTNT-DPP series

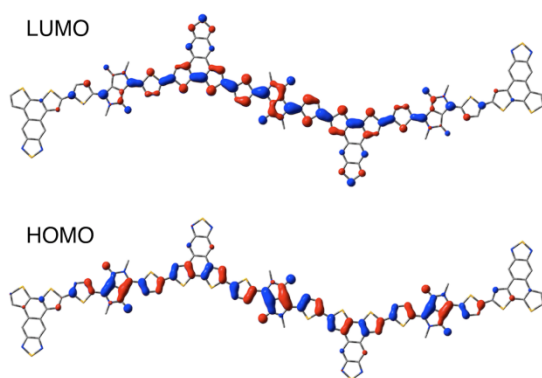


**Figure 7.** Frontier orbitals of PDTNT-BTh (a) and PDTNT-DPP (b) series and assignment of the transitions of each absorption band obtained from TD-DFT calculations at the B3LYP/6-311G(d,p) level of theory.

To gain further insights into the electronic structure of the polymers, DFT studies were conducted at the B3LYP/6-31G(d) level for geometry optimization obtained with the Gaussian 09 program. TD-DFT was performed on the optimized structure with the B3LYP/6-311G(d,p) level to provide the first 10 excited states.

Oligomer systems with DTNT at the terminal ends were used for the calculation, and the solubilizing substituents were replaced with a methyl group for ease of calculation. The frontier orbitals obtained from the calculations are shown in Figure 7. In PDTNT-BTh, the calculated dihedral angle between two mean planes of methylthiophenes was  $2^\circ$ , while that between DTNT and methylthiophene was  $19^\circ$  due to the steric hindrance caused by the methyl group in the  $\beta$  position of thiophene in a neighboring DTNT. In PDTNT-DPP, the polymer had a planar structure with a dihedral angle of  $0^\circ$  for the mean planes between diketopyrrolopyrrole and thiophene moieties and  $1^\circ$  between thiophene and DTNT moieties.

In PDTNT-BTh, the HOMO was delocalized over the polymer backbone, whereas the LUMO was localized on the DTNT moieties at the center of the polymer. Based on the TD-DFT calculations, the absorption shoulder (the longest absorption band) can be attributed to the HOMO to LUMO transition. On the other hand, in PDTNT-DPP, the HOMO and the LUMO orbitals were delocalized over its backbone. The strongest absorption can be assigned to the HOMO–LUMO transition. While the calculations predict a strong charge transfer character for the

HOMO–LUMO transition of PDTNT-BTh, the experimental absorption energies are much higher than those for the PDTNT-DPP polymers.

## Photovoltaic performance

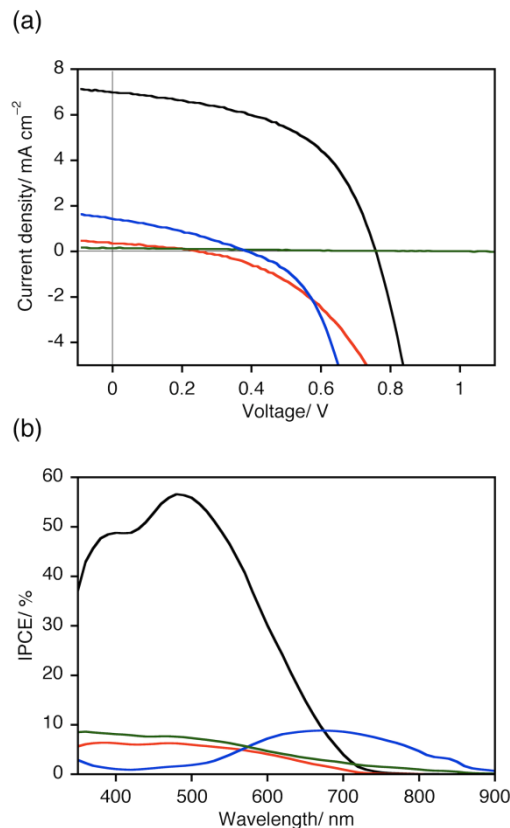


**Figure 8.**  $J$ - $V$  curves (a) and IPCE spectra (b) of the polymer-based OPV cells for PDTNT-BThEH/PC<sub>71</sub>BM (black), PDTNT-BThOD/PC<sub>71</sub>BM (red), PDTNT-DPPOD/PC<sub>71</sub>BM (green) and PDTNT-DPPOD/C<sub>60</sub> (blue). The IPCE spectrum in green is obtained from the six OPV cells connected in parallel.

Table 4. Photovoltaic properties of the polymer/fullerene blend cells

polymer	fullerene	weight ratio	$J_{SC}/\text{mA cm}^{-2}$	$V_{OC}/\text{V}$	$FF$	PCE
PDTNT-BThEH	PC <sub>71</sub> BM	1:1	6.98	0.758	0.52	2.76
PDTNT-BThOD	PC <sub>71</sub> BM	1:1	0.35	0.245	0.22	0.019
PDTNT-DPPOD	PC <sub>71</sub> BM	1:1	0.23	1.08	0.10	0.025
PDTNT-DPPOD	C <sub>60</sub>	1:1	1.46	0.378	0.33	0.182

The photovoltaic properties of the polymers were evaluated with the optimized cell structures of ITO/PEDOT:PSS (40 nm)/polymer:fullerene/HBL/Al (80 nm) under AM1.5G conditions. For optimized PDTNT-BThEH and PDTNT-DPPOD, Ca (20 nm) was used as the hole blocking layer, and in the case of PDTNT-BThOD, a blocking layer was not used. Active layers were prepared from *o*DCB for PDTNT-BThEH and from CB for PDTNT-BThOD and PDTNT-DPPOD with appropriate concentrations of 1:1 mixtures of polymer and fullerene. The active layers were obtained as amorphous films. OPV cells could not be fabricated with PDTNT-DPPEH because it was not sufficiently soluble in CB or *o*DCB for the cell

fabrication process. The  $J$ - $V$  curves, IPCE spectra, and photovoltaic characteristics of the best devices are displayed in Figure 8 and Table 4. **PDTNT-BThEH**, which has short branched alkyl chain, showed the highest PCE of the investigated cells with a value of 2.76% and a  $J_{SC}$  of 6.98 mA cm<sup>-2</sup>, a  $V_{OC}$  of 0.76 V, and a fill factor ( $FF$ ) of 0.52. On the other hand, **PDTNT-BThOD** and **PDTNT-DPPOD**, which have a long branched alkyl chain, did not exhibit effective power conversion. The low PCE value obtained for **PDTNT-BThOD** and **PDTNT-DPPOD** could be caused by the low molecular weight of the polymers, which in turn could not lead to the migration of charge carriers among the polymer backbone. Furthermore, large alkyl chains only enhance polymer solubility; they do not contribute to light harvesting and charge transfer. The IPCE spectrum of the cell prepared with **PDTNT-BThEH** covered a broad wavelength range from 350 to 700 nm with an IPCE maximum of 57% at 480 nm and a shoulder at 400 nm (49%). These values are in good agreement with the UV spectrum of the **PDTNT-BThEH** film. The **PDTNT-BThOD** cell showed a weaker but similar spectrum to the ethylhexyl system, with peaks observed at 380 and 470 nm. The IPCE spectrum of the **PDTNT-DPPOD** cell (green line in Figure 8b) was different from the UV-Vis spectrum of the films but similar to that of PC<sub>71</sub>BM, indicating that electron transfer did not occur between **PDTNT-DPPOD** and PC<sub>71</sub>BM. In this case, however, only hole transfer did occur. The replacement of PC<sub>71</sub>BM with C<sub>60</sub>, which has a lower LUMO energy, led to an IPCE spectrum (blue line in Figure 8b) that was similar to the UV-Vis spectrum of the **PDTNT-DPPOD** film, with a maximum absorption at 670 nm. The result suggests that both electron and hole transfer occurred between **PDTNT-DPPOD** and C<sub>60</sub>.

## Conclusions

The control of the absorption band and a narrow band gap with low HOMO and LUMO energies were achieved in two out of the four polymers based on T-shaped DTNT, which consists of donor and acceptor moieties fused through a naphthalene ring. DTNT could not be converted to the precursor for Suzuki or Stille coupling, and tried polymerizations with a C—H activated direct arylation technique, even though the reaction can possibly take place at not only  $\alpha$  positions but also  $\beta$  positions to give rise to a cross-linking polymer. Electrochemical study results showed that DTNT acts as both an electron donor and an electron acceptor, revealing the ambipolar nature of the DTNT. The copolymers with bithiophene as a counterpart, i.e., **PDTNT-BThEH** and **PDTNT-BThOD**, showed three clear absorption bands in the UV-Vis spectra. The combination of a strong electron acceptor (DPP) and DTNT afforded narrow band gap polymers (**PDTNT-DPPEH** and **PDTNT-DPPOD**) with a band gap energy of ~1.4 eV and low HOMO energy of -5.43 eV. Electron transfer did not occur between **PDTNT-DPPOD** and PC<sub>71</sub>BM, resulting in poor PCE performance. However, electron transfer did occur between **PDTNT-DPPOD** and C<sub>60</sub> to exhibit higher PCE performance. The best photovoltaic performance was obtained in an OPV cell with a 1:1 blend ratio of **PDTNT-BThEH**/PC<sub>71</sub>BM, which gave a  $J_{SC}$  of 6.98 mA/cm<sup>-2</sup>, a  $V_{OC}$  of 0.758 V, a  $FF$  of 0.52 and a PCE of 2.76%. We are in progress in preparation of soluble ambipolar monomer units for general polymerization procedures.

## Experimental

### General

All chemicals were purchased from commercial suppliers (Wako Pure Chemical, TCI, Kanto Chemical Co. Inc., and Aldrich) and

used as received unless stated otherwise. Air- and moisture-sensitive reactions were conducted under an argon atmosphere using standard Schlenk techniques. THF (deoxidized, Wako Pure Chemical) was used for the electrochemical measurement of DTNT. DMAc (dehydrated, Wako Pure Chemical) was used for polymer syntheses. Column chromatography was conducted using silica gel N60 (spherical, neutralized) with a particle size of 40–50  $\mu$ m from Kanto Chemical Co. Inc. Size exclusion chromatography was carried out using Bio-Beads® S-X1 and S-X3 Beads (Bio-Rad) with THF as the eluent.

### Instruments

Automated column chromatography was performed on an EPCLC-W-Prep 2XY A-Type apparatus (YAMAZEN) with cartridges HI-FLASH™ Column packed with 40  $\mu$ m of silica gel. Preparative gel permeation chromatography (GPC) was performed on an LC-9201 system (Japan Analytical Industry Co. Ltd.) equipped with two columns (JAIGEL-1H and JAIGEL-2H). NMR spectra were recorded on a JNM-ECA400 spectrometer (JEOL Resonance). Chemical shifts in CDCl<sub>3</sub> were calibrated using residual chloroform (CHCl<sub>3</sub>) at 7.26 ppm for <sup>1</sup>H NMR and 77.16 ppm for <sup>13</sup>C NMR.<sup>27</sup> UV-Vis spectral measurements were performed on a V-570 spectrophotometer (JASCO Corporation) for solution and thin films, and an integrating sphere was attached to measure the reflectance spectrum of crystalline-state DTNT. The electronic spectra in the reflectance mode were converted to absorbance spectra in accordance with the Lambert–Beer law. Cyclic voltammetry (CV) was conducted on a Compactstat system with IviumSoft (Ivium technologies) under an argon flow. TBAPF<sub>6</sub> (0.1 M) was used as a supporting electrolyte. A conventional three-electrode cell was used with a platinum (Pt) working electrode and a Pt wire as the counter electrode. The potentials were measured with respect to the Ag/AgNO<sub>3</sub> (0.01 M acetonitrile solution containing 0.1 M of tetrabutylammonium perchlorate; TBAP) reference electrode. Potentials (vs Ag/Ag<sup>+</sup>) were converted to the values vs Fc/Fc<sup>+</sup> by subtracting 0.05 V. The shifted value was estimated from the redox potential of Fc/Fc<sup>+</sup> in DCM,<sup>27,26</sup> and the redox potentials of Ag/Ag<sup>+</sup> and Ag/AgCl couples vs standard hydrogen electrode.<sup>29</sup> To estimate molecular weights, analytical GPC was conducted on a Shodex GPC-101 (Showa-Denko) equipped with a guard column (Shodex GPC KF-G), and two 30-cm columns (KF-803 and KF-804) with an internal differential refractive index detector. Samples were eluted with THF at 40 °C at a flow rate of 0.8 mL min<sup>-1</sup>, and the system was calibrated with polystyrene standards. The HOMO energies of the films were estimated by photoelectron spectroscopy in air (PESA) on an AC-3 photoemission yield spectrometer (RIKEN KEIKI).<sup>30</sup> Theoretical calculations based on density functional methods were performed with the Gaussian09 program.<sup>31</sup> Becke's three-parameter<sup>32</sup> gradient-corrected functional (B3LYP) with 6-31G(d) basis was used for the geometry optimizations and vibrational frequency analyses. Time dependent-DFT (TD-DFT) calculation and energy optimization was conducted at B3LYP/6-311G(d,p) basis set. The obtained geometry and frontier orbitals were depicted with a GaussView 5 program.<sup>33</sup> High-resolution mass spectrometry was performed at the Instrumental Analysis Division, Equipment Management Center, Creative Research Institution, Hokkaido University.

### Fabrication and Characterization of OPVs

The OPV cells were fabricated in the following configuration: ITO/PEDOT:PSS/active layer/HBL/Al. The patterned ITO (conductivity: 15  $\Omega$  square<sup>-1</sup>) glass was precleaned in an

ultrasonic bath with detergent, water, and 2-propanol and then treated in an ultraviolet-ozone chamber. A thin layer (40 nm) of PEDOT:PSS was spin coated at 5000 rpm and subsequently dried at 140 °C for 10 min on a hot plate under air. In an N<sub>2</sub> glove box, a CB or *o*DCB solution of the polymer and fullerene blend was spin coated onto the PEDOT:PSS surface to form the active layer. For the device with C<sub>60</sub>, *o*DCB was used. The thicknesses of the blend films and PEDOT:PSS layers were measured using a Dektak 6M stylus profiler (Veeco Instruments Inc.). Thermal evaporation of Al (80 nm) electrode with or without Ca (20 nm) hole blocking layer at a chamber pressure of less than 1 × 10<sup>-4</sup> Pa resulted in the final devices. This process provided devices with an active area of 1.5 × 4 mm<sup>2</sup> and they are sealed using UV-curable resins before the subsequent measurements in ambient conditions. The current density–voltage (*J*–*V*) curves were measured using an ADCMT 6244 DC voltage current source/monitor under AM 1.5G solar simulated light irradiation of 100 mW cm<sup>-2</sup> with a WXS-90S-L2 Super solar simulator (Wacom Electric Co. Ltd.) using an aperture mask of 0.0435 cm<sup>2</sup>. Photocurrent action spectra and incident photon-to-current conversion efficiency (IPCE) were measured using a CEP-2000 system (Bunkoukeiki Co. Ltd.).

## Synthesis

### 5,6-Di(thiophen-3-yl)benzo[*c*][1,2,5]thiadiazole (1)

5,6-Dibromo-2,1,3-benzothiadiazole (6.53 g, 22.2 mmol) and 3-thiopheneboronic acid (6.28 g, 49.0 mmol) were dissolved in dioxane (150 mL) and a solution of potassium carbonate (20.3 g, 147 mmol) in water (60 mL) was added. Ar was bubbled through the reaction mixture for 20 min, and palladium acetate (502 mg, 2.2 mmol) and tri(*o*-tolyl)phosphine (1.36 g, 4.5 mmol) were added. The reaction mixture was heated at 100 °C overnight. The mixture was cooled to room temperature, dichloromethane (DCM) was added, and the organic phase was washed three times with water. The organic layer was dried over magnesium sulfate, and the solvent was removed under reduced pressure. The crude product was purified by silica gel column chromatography (2:1 hexane/DCM as eluent) to give a pale yellow solid (5.87 g, 88%). <sup>1</sup>H NMR (400 MHz, CDCl<sub>3</sub>) δ (ppm): 8.04 (s, 2H), 7.23 (dd, *J* = 4.8, 2.4 Hz, 2H), 7.18 (m, 2H) 6.81 (dd, *J* = 5.2, 1.2 Hz, 2H). <sup>13</sup>C NMR (100 MHz, CDCl<sub>3</sub>) δ (ppm): 154.44, 140.85, 138.56, 128.88, 125.45, 124.23, 121.42. HRMS (APCI) *m/z* calcd for C<sub>14</sub>H<sub>9</sub>N<sub>2</sub>S<sub>3</sub> 300.9922, found 300.9919.

### Dithieno[3'2':5,6;2'',3'':7,8]naphtho[2,3-*c*][1,2,5]thiadiazole (DTNT, 2)

Ar was bubbled through a solution of **1** (1.24 g, 4.1 mmol) in DCM (500 mL) for 15 min. Ar was bubbled through a solution of iron(III) chloride (1.49 g, 9.18 mmol) in nitromethane (30 mL) for 15 min, and this solution was added to the reaction mixture. The mixture was stirred for 2 h, and methanol (100 mL) was added. The solvent was evaporated under reduced pressure. The crude product was passed through a plug of silica gel with DCM, and the product was purified by silica gel column chromatography (1:1 hexane/DCM as eluent) to afford a red powder (698 mg, 57%). <sup>1</sup>H NMR (400 MHz, CDCl<sub>3</sub>) δ (ppm): 8.98 (s, 2H), 8.05 (d, *J* = 5.2 Hz, 2H), 7.54 (d, *J* = 4.8 Hz, 2H). <sup>13</sup>C NMR (100 MHz, CDCl<sub>3</sub>) δ (ppm): 152.75, 134.10, 133.47, 130.62, 124.47, 123.93, 115.16. HRMS (APCI) *m/z* calcd for C<sub>14</sub>H<sub>7</sub>N<sub>2</sub>S<sub>3</sub> 298.9766, found 298.9768. UV-vis (extinction coefficient in *o*DCB as 10<sup>3</sup>ε/ M<sup>-1</sup>cm<sup>-1</sup> are listed in parentheses): 320 (12), 368 (15), 386 (19), 449 (3.4).

### PDTNT-BTheH

A mixture of **2** (246 mg, 0.82 mmol), **8** (452 mg, 0.82 mmol), 1-adamantane carboxylic acid (45 mg, 0.25 mmol), potassium

carbonate (288 mg, 2.1 mmol), and palladium acetate (5.5 mg, 0.024 mmol) in a 50 mL round-bottom flask was purged with argon for 15 min. DMAc (8.2 mL) was added, and the mixture was stirred at 100 °C for 24 h. The mixture was cooled to room temperature, and poured into methanol (300 mL) using a minimum amount of CF. The precipitate was filtrated using a membrane filter (0.45 mm) and successively extracted using a Soxhlet apparatus with hexane, acetone, and CF. The CF fraction was concentrated, dissolved in the minimum amount of CF, and poured into methanol (300 mL). The precipitate was collected on a membrane filter (0.45 mm) and dried under vacuum to give a brown powder (272 mg, 48%). <sup>1</sup>H NMR (400 MHz, CDCl<sub>3</sub>) δ (ppm): 9.01–8.50 (m, br, 2H), 8.11–7.64 (m, br, 2H), 7.21–6.79 (m, br, 2H), 2.98–2.39 (m, br, 4H), 1.90–1.72 (s, br, 2H), 1.51–1.16 (s, br, 16H), 1.05–0.78 (s, br, 12H).

### PDTNT-BThOD

A mixture of **2** (138 mg, 0.46 mmol), **9** (409 mg, 0.46 mmol), 1-adamantane carboxylic acid (25 mg, 0.014 mmol), potassium carbonate (162 mg, 1.2 mmol), and palladium acetate (3.7 mg, 0.016 mmol) in a 50 mL round-bottom flask was purged with argon for 15 min. DMAc (4.6 mL) was added, and the mixture was stirred at 100 °C for 24 h. The mixture was cooled to room temperature and poured into methanol (300 mL) using minimum amount of CF. The precipitate was passed through a column of Bio-Beads<sup>®</sup>, first with an exclusion limit of 16000 and then with a limit of 2000 using CF as eluent. After solvent removal, the residue was dissolved in a small amount of CF and poured into methanol (300 mL). The precipitate was filtrated using a membrane filter (0.45 mm) and dried under vacuum to give a brown powder (333 mg, 70%). <sup>1</sup>H NMR (400 MHz, CDCl<sub>3</sub>) δ (ppm): 9.02–8.40 (m, br, 2H), 8.10–7.53 (m, br, 2H), 7.18–6.79 (m, br, 2H), 2.99–2.36 (m, br, 4H), 1.91–1.78 (s, br, 2H), 1.50–1.07 (m, br, 62H), 0.92–0.75 (m, br, 12H).

### PDTNT-DPPEH

A mixture of **2** (198 mg, 0.66 mmol), **14** (452 mg, 0.66 mmol), 1-adamantane carboxylic acid (36 mg, 0.20 mmol), potassium carbonate (230 mg, 1.7 mmol), and palladium acetate (7.7 mg, 0.034 mmol) in a 50 mL round-bottom flask was purged with argon for 15 min. DMAc (6.6 mL) was added, and the mixture was stirred at 100 °C for 24 h. The mixture was cooled to room temperature and poured into methanol (200 mL) using the minimum amount of CF required to maintain fluidity. The precipitate was filtered using a membrane filter (0.45 mm) and successively extracted using a Soxhlet apparatus with hexane, acetone, CF, and CB. The CB fraction was concentrated and poured into methanol (200 mL) to give a dark blue powder (89 mg, 16%). The <sup>1</sup>H NMR spectrum of PDTNT-DPPEH could not be recorded because of low solubility in CDCl<sub>3</sub>.

### PDTNT-DPPOD

A mixture of **2** (181 mg, 0.61 mmol), **15** (618 mg, 0.61 mmol), 1-adamantane carboxylic acid (37 mg, 0.21 mmol), potassium carbonate (203 mg, 2.0 mmol), and palladium acetate (5.4 mg, 0.024 mmol) in a 50 mL round-bottom flask was purged with argon for 15 min. DMAc (12 mL) was added, and the mixture was stirred at 100 °C for 24 h. The mixture was cooled to room temperature and poured into methanol (300 mL) using minimum amount of CF required to maintain fluidity. The precipitate was filtered using a membrane filter (0.45 mm) and successively extracted using a Soxhlet apparatus with hexane, acetone, and CF. The CF fraction was concentrated, dissolved in a minimum amount of CF and poured into methanol (300 mL). The precipitate was collected on a membrane filter (0.45 mm) and dried under vacuum to give a dark blue powder (487 mg, 69%). <sup>1</sup>H NMR (400 MHz, CDCl<sub>3</sub>) δ (ppm): 9.42–6.87 (m, br, 8H),

4.52–3.66 (s, br, 4H), 2.15–1.79 (s, br, 2H), 1.64–1.06 (m, br, 62H), 0.93–0.72 (m, br, 12H).

## Acknowledgement

This work was supported by a MEXT Program for Development of Environmental Technology using Nanotechnology and a Giant-in Aid for Scientific Research (No.25810080) from the JSPS.

## Notes and references

† Electronic Supplementary Information (ESI) available: Details of synthesis of compounds 3–15, UV-Vis spectra of PDTNT-BThEH and PDTNT-DPPEH in oDCB and film, details of molecular orbitals of DTNT, PDTNT-BTh, and PDTNT-DPP, selected results of the TD-DFT excited state transitions for DTNT, PDTNT-BTh, and PDTNT-DPP, and the <sup>1</sup>H and <sup>13</sup>C NMR spectra of compounds 1–15. See DOI: 10.1039/b000000x/

- (a) H. Spanngaard and F. C. Krebs, *Sol. Energy Mater. Sol. Cells*, 2004, **83**, 125; (b) S. Gunes, H. Neugebauer and N. S. Saricifti, *Chem. Rev.*, 2007, **107**, 1324; (c) B. C. Thompson and J. M. J. Fréchet, *Angew. Chem., Int. Ed.*, 2008, **47**, 58; (d) G. Dennler, M. C. Scharber and C. J. Brabec, *J. Adv. Mater.*, 2009, **21**, 1323; (e) F. G. Brunetti, R. Kumar and F. Wudl, *J. Mater. Chem.*, 2010, **20**, 2934; (f) Y. Liang and L. Yu, *Acc. Chem. Soc.*, 2010, **43**, 1227; (g) G. Li, R. Zhu and Y. Yang, *Nat. Photonics*, 2012, **6**, 153; (h) M. Mayukh, I. H. Jung, F. He and L. Yu, *J. Polym. Sci. B: Polym. Phys.*, 2012, **50**, 1057; (i) Y. Li, *Acc. Chem. Res.*, 2012, **45**, 723; (j) H. J. Son, B. Carsten, I. H. Jung and L. Yu, *Energy Environ. Sci.*, 2012, **5**, 8158; (k) C. Duan, F. Huang and Y. Cao, *J. Mater. Chem.*, 2012, **22**, 10416; (l) L. Dou, J. You, Z. Hong, Z. Xu, G. Li, R. A. Street and Y. Yang, *Adv. Mater.*, 2013, **25**, 6642.
- (a) C. J. Brabec and J. R. Durrant, *MRS Bull.*, 2008, **33**, 670; (b) F. C. Krebs, *Sol. Energy Mater. Sol. Cells*, 2009, **93**, 394; (c) F. C. Krebs, T. Tromholt and M. Jørgensen, *Nanoscale*, 2010, **2**, 873; (d) R. Søndergaard, M. Hösel, D. Angmo, T. T. Larsen-Olsen and F. C. Krebs, *Mater. Today*, 2012, **15**, 36; (e) A. Teichler, J. Perelaer and U. S. Schbert, *J. Mater. Chem. C*, 2013, **1**, 1910; (f) Y. Sun, Y. Zhang, Q. Liang, Y. Zhang, H. Chi, Y. Shi and D. Fang, *RSC Advances*, 2013, **3**, 11925; (g) R. Po, A. Bernardi, A. Calabrese, C. Carbonera, G. Corso and A. Pellegrino, *Energy Environ. Sci.*, 2014, **7**, 925.
- (a) J. You, L. Dou, K. Yoshimura, T. Kato, K. Ohya, T. Moriarty, K. Emery, C.-C. Chen, J. Gao, G. Li and Y. Yang, *Nature Commun.*, 2013, **4**, 1446; (b) J. You, C.-C. Chen, Z. Hong, K. Yoshimura, K. Ohya, R. Xu, S. Ye, J. Gao, G. Li and Y. Yang, *Adv. Mater.*, 2013, **1**, 3973; (c) M. A. Green, K. Emery, Y. Hishikawa, W. Warta and E. D. Dunlop, *Prog. Photovoltaics*, 2014, **22**, 1.
- (a) D. Mühlbacher, M. Scharber, M. Morana, Z. Zhu, D. Waller, R. Gaudiana and C. J. Brabec, *Adv. Mater.*, 2006, **18**, 2884; (b) L. Huo, J. Hou, H.-Y. Chen, S. Zhang, Y. Jiang, T. L. Chen and Y. Yang, *Macromolecules*, 2009, **42**, 6564; (c) M. Wang, X. Hu, P. Liu, W. Li, X. Gong, F. Huang and Y. Cao, *J. Am. Chem. Soc.*, 2011, **133**, 9638; (d) C. M. Amb, S. Chen, K. R. Graham, J. Subbiah, C. E. Small, F. So and J. R. Reynolds, *J. Am. Chem. Soc.*, 2011, **133**, 10062; (e) E. Wang, Z. Ma, Z. Zhang, K. Vandewal, P. Henriksson, O. Inganäs, F. Zhang and M. R. Andersson, *J. Am. Chem. Soc.*, 2011, **133**, 14244; (f) L. Dou, C.-C. Chen, K. Yoshimura, K. Ohya, W.-H. Chang, J. Gao, Y. Liu, E. Richard and Y. Yang, *Macromolecules*, 2013, **46**, 3384; (g) S. Zhang, L. Ye, Q. Wang, Z. Li, L. Guo, H. Fan and J. Hou, *J. Phys. Chem. C*, 2013, **117**, 9550.
- (a) M. C. Scharber, D. Mühlbacher, M. Koppe, P. Denk, C. Waldauf, A. J. Heeger and C. J. Brabec, *Adv. Mater.*, 2006, **18**, 789; (b) Y. J. He, H.-Y. Chen, H. Hou and Y. Li, *J. Am. Chem. Soc.*, 2010, **132**, 1377; (c) Y. He, G. Zhao, B. Peng and Y. Li, *Adv. Funct. Mater.*, 2010, **20**, 3383.

- (a) J. M. Szarko, J. Guo, Y. Liang, B. Lee, B. S. Rolczynski, J. Strzalka, T. Xu, S. Loser, T. J. Marks, L. Yu and L. X. Chen, *Adv. Mater.*, 2010, **22**, 5468; (b) A. T. Yiu, P. M. Beaujuge, O. P. Lee, C. H. Woo, M. F. Toney and J. M. J. Fréchet, *J. Am. Chem. Soc.*, 2012, **134**, 2180; (c) T.-Y. Chu, J. Lu, S. Beaupré, Y. Zhang, J.-R. Pouliot, J. Zhou, A. Najari, M. Leclerc and Y. Tao, *Adv. Funct. Mater.*, 2012, **22**, 2345; (d) T. Nakanishi, Y. Shirai, T. Yasuda and L. Han, *J. Polym. Sci. A: Polym. Chem.*, 2012, **50**, 4829; (e) C. Cabanetos, A. E. Labban, J. A. Bartelt, J. D. Douglas, W. R. Mateker, J. M. J. Fréchet, M. D. McGehee and P. M. Beaujuge, *J. Am. Chem. Soc.*, 2013, **135**, 4656; (f) I. Osaka, M. Saito, T. Koganezawa and K. Takimiya, *Adv. Mater.*, 2014, **26**, 331.
- (a) J. K. Lee, W. L. Ma, C. J. Brabec, J. Yuen, J. S. Moon, J. Y. Kim, K. Lee, G. C. Bazan and A. J. Heeger, *J. Am. Chem. Soc.*, 2008, **130**, 3619; (b) J. T. Roger, K. Schmidt, M. F. Toney, E. J. Kramer and G. C. Bazan, *Adv. Mater.*, 2011, **23**, 2284; (c) M.-S. Su, C.-Y. Kuo, M.-C. Yuan, U.-S. Jeng, C.-J. Su and K.-H. Wei, *Adv. Mater.*, 2011, **23**, 3315; (d) X. Liu, S. Huettner, Z. Rong, M. Sommer and R. H. Friend, *Adv. Mater.*, 2012, **24**, 669; (e) K. Schmidt, C. J. Tassone, J. R. Niskala, A. T. Yiu, O. P. Lee, T. M. Weiss, C. Wang, J. M. J. Fréchet, P. M. Beaujuge and M. F. Toney, *Adv. Mater.*, 2014, **26**, 300.
- (a) S. Honda, H. Ohkita, H. Benten and S. Ito, *Adv. Energy Mater.*, 2011, **1**, 588; (b) E. Lim, S. Lee and K. K. Lee, *Chem. Commun.*, 2011, **47**, 914; (c) T. Ameri, J. Min, N. Li, F. Machui, D. Baran, M. Forster, K. J. Schottler, D. Dolfen, U. Scherf and C. J. Brabec, *Adv. Energy Mater.*, 2012, **2**, 1198; (d) L. Yang, H. Zhou, S. C. Price and W. You, *J. Am. Chem. Soc.*, 2012, **134**, 5432; (e) Y.-C. Chung, C.-Y. Hsu, R. Y.-Y. Lin, K.-C. Ho and J. T. Lin, *ChemSusChem*, 2013, **6**, 20. (f) H. Cha, D. S. Chung, S. Y. Bae, M.-J. Lee, T. K. An, J. Hwang, K. H. Kim, Y.-H. Kim, D. H. Choi and C. E. Park, *Adv. Funct. Mater.*, 2013, **23**, 1556; (g) T. Ameri, P. Khoram, J. Min and C. J. Brabec, *Adv. Mater.*, 2013, **25**, 4245; (h) J. Min, T. Ameri, R. Gresser, M. Lorenz-Rothe, D. Baran, A. Troeger, V. Sgobba, K. Leo, M. Riede, D. M. Guldi and C. J. Brabec, *ACS Appl. Mater. Interfaces*, 2013, **5**, 5609.
- (a) J. Roncali, *Chem. Rev.*, 1997, **97**, 173; (b) M. Pomerantz, in *Handbook of Conducting Polymers*, eds. T. A. Skotheim, R. L. Eisenbaumer and J. R. Reynolds, Marcel Dekker, Inc., New York, 2nd edn, 1998, ch.11; (c) S. C. Rasmussen and M. Pomerantz, in *Handbook of Conducting Polymers*, eds. T. A. Skotheim and J. R. Reynolds, CRC Press, Boca Raton, FL, 2007, ch. 12, vol. 1; (d) S. C. Rasmussen, K. Ogawa and S. D. Rothstein, in *Handbook of Organic Electronics and Photonics*, ed. H. S. Nalwa, American Scientific Publishers, Stevenson Ranch, CA, 3rd edn, 2008, ch. 1, vol. 1; (e) S. C. Rasmussen, R. L. Schwiderski and M. E. Mulholland *Chem. Commun.*, 2011, **47**, 11394.
- (a) Y. Liang, D. Feng, Y. Wu, S.-T. Tsai, G. Li, C. Ray and L. Yu, *J. Am. Chem. Soc.*, 2009, **131**, 7792; (b) N. Kleinhenz, L. Yang, H. Zhou, S. C. Price and W. You, *Macromolecules*, 2011, **44**, 872; (c) L. Huo, S. Zhang, Z. Guo, F. Xu, Y. Li and J. Hou, *Angew. Chem., Int. Ed.*, 2011, **50**, 9697; (d) B. Carsten, J. M. Szarko, H. J. Son, W. Wang, L. Lu, F. He, B. S. Rolczynski, S. J. Lou, L. X. Chen and L. Yu, *J. Am. Chem. Soc.*, 2011, **133**, 20468.
- (a) W. A. Braunecker, Z. R. Owczarczyk, A. Garcia, N. Kopidakis, R. E. Larsen, S. R. Hammond, D. S. Ginley and D. C. Olson, *Chem. Mater.*, 2012, **24**, 1346; (b) Y. Ie, J. Huang, Y. Uetani, M. Karakawa and Y. Aso, *Macromolecules*, 2012, **45**, 4564; (c) W. Wu, Y. Jing, Z. Guo, S. Zhang, M. Zhang, L. Huo and J. Hou, *Polym. Chem.*, 2013, **4**, 536; (d) W. Yue, T. T. Larsen-Olsen, X. Hu, M. Shi, H. Chen, M. Hinge, P. Fojan, F. C. Krebs and D. Yu, *J. Mater. Chem. A*, 2013, **1**, 1785; (e) S.-O. Kim, Y.-S. Kim, H.-J. Yun, I. Kang, Y. Yoon, N. Shin, H. J. Son, H. Kim, M. J. Ko, B. Kim, Y.-H. Kim and S.-K. Kwon, *Macromolecules*, 2013, **46**, 3861; (f) W. Cui and F. Wudl, *Macromolecules*, 2013, **46**, 7232; (g) W. Yue, X. Huang, J. Yuan, W. Ma, F. C. Krebs and D. Yu, *J. Mater. Chem. A*, 2013, **1**, 10116. (h) J. Huang, Y. Ie, M. Karakawa and Y. Aso, *J. Mater. Chem. A*, 2013, **1**, 15000.
- S. Rasmussen, in *Low Bandgap Polymers*, eds. S. Kobayashi and K. Müllen, SpringerReference, Springer-Verlag, Berlin, Heidelberg, 2013.

- 13 L. Pandey, C. Risko, J. E. Norton and J.-L. Brédas, *Macromolecules*, 2012, **45**, 6405.
- 14 P. M. Beaujuge, C. M. Amb and J. R. Reynolds, *Acc. Chem. Res.*, 2010, **43**, 1396.
- 5 15 (a) H. Fan, Z. Zhang, Y. Li and Z. Zhan, *J. Polym. Sci. A: Polym. Chem.*, 2011, **49**, 1462; (b) P. Shen, H. Bin, L. Xiao and Y. Li, *Macromolecules*, 2013, **46**, 9575.
- 16 (a) H.-Y. Chen, J. Hou, S. Zhang, Y. Liang, G. Yang, L. Yu, Y. Wu and G. Li, *Nat. Photonics*, 2009, **3**, 649; (b) S. C. Price, A. C. Stuart, L. Yang, H. Zhou and W. You, *J. Am. Chem. Soc.*, 2011, **133**, 4625; (c) H.-C. Chen, Y.-H. Chen, C.-C. Liu, Y.-C. Chien, S.-W. Chou and P.-T. Chou, *Chem. Mater.*, 2012, **24**, 4766; (d) J. Min, Z.-G. Zhang, M. Zhang and Y. Li, *Polym. Chem.*, 2013, **4**, 1467; (e) A. C. Stuart, J. R. Tumbleston, H. Zhou, W. Li, S. Liu, H. Ade and W. You, *J. Am. Chem. Soc.*, 2013, **135**, 1806; (f) J.-F. Jheng, Y.-Y. Lai, J.-S. Wu, Y.-H. Chao, C.-L. Wang and C.-S. Hsu, *Adv. Mater.*, 2013, **25**, 2445; (g) X. Wang, Z.-G. Zhang, H. Luo, S. Chen, S. Yu, H. Wang, X. Li, G. Yu and Y. Li, *Polym. Chem.*, 2014, **5**, 502.
- 17 (a) M. Seri, M. Blognesi, Z. Chen, S. Lu, W. Koopman, A. Facchetti and M. Muccini, *Macromolecules*, 2013, **46**, 6419; (b) J. A. Clement, H. G. Kim, M. Sim, B. Kang and K. Cho, *RSC Adv.*, 2013, **3**, 6799.
- 18 X. Hu, L. Zuo, W. Fu, T. T. Larsen-Olsen, M. Helgesen, E. Bundgaard, O. Hagemann, M. Shi, F. C. Krebs and H. J. Chen, *Mater. Chem.*, 2012, **22**, 15710.
- 25 19 (a) H. Zhou, L. Yang, S. C. Price, K. J. Knight and W. You, *Angew. Chem., Int. Ed.*, 2010, **49**, 7992; (b) Y. Zhang, J. Zou, H.-L. Yip, K.-S. Chen, J. A. Davis, Y. Sun and A. K.-U. Jen, *Macromolecules*, 2011, **44**, 4752; (c) C. P. Yau, Z. Fei, R. S. Ashraf, M. Shahid, S. E. Watkins, P. Pattanasattayavong, T. D. Anthopoulos, V. G. Gregoriou, C. L. Chochos and M. Heeney, *Adv. Funct. Mater.*, 2014, **24**, 678.
- 20 (a) Mulholland, M. E.; Schwiderski, R. L.; Evenson, S. J.; Rasmussen, S. C., *Polym. Mat. Sci. Eng.*, 2012, **107**, 36.; (b) Wen, Li; Heth, Christopher L.; Rasmussen, Seth C., *Phys. Chem. Chem. Phys.*, 2014, **16**, 7231.
- 35 21 R. N. Jones, *Chem. Rev.*, 1947, **41**, 353.
- 22 J. Tanaka, *Bull. Chem. Soc. Jpn.*, 1965, **38**, 86.
- 23 V. S. Reddy, S. Karak, S. K. Ray and A. Dhar, *J. Phys D: Appl. Phys.*, 2009, **42**, 145103.
- 24 (a) F. Bellina and R. Rossi, *Tetrahedron*, 2009, **65**, 10269; (b) L. Ackermann, R. Vicente and A. R. Kapdi, *Angew. Chem., Int. Ed.*, 2009, **48**, 9792. (c) L. Ackermann, *Chem. Rev.*, 2011, **111**, 1315.
- 25 (a) M. Sévignon, J. Papillon, E. Schulz and M. Lemaire *Tetrahedron Lett.*, 1999, **40**, 5873; (b) Q. F. Wang, R. Takita, Y. Kikuzaki and F. Ozawa, *J. Am. Chem. Soc.*, 2010, **132**, 11420; (c) Y. Fujinami, J. Kuwabara, W. Lu, H. Hayashi and T. Kanbara, *ACS Macro Lett.*, 2012, **1**, 67. (d) J. Jo, A. Pron, P. Berrouard, W. L. Leong, J. D. Yuen, J. S. Moon, M. Leclerc and A. J. Heeger, *Adv. Emergy Mater.*, 2012, **2**, 1397; (e) P. Berrouard, A. Najari, A. Pron, D. GEndron, P.-O. Morin, J.-R. Pouliot, J. Leilleux and M. Leclerc, *Angew. Chem., Int. Ed.*, 2012, **51**, 2068; (f) A. Facchetti, L. Vaccaro and A. Marrocchi, *Angew. Chem., Int. Ed.*, 2012, **51**, 3520; (g) K. Yamazaki, J. Kuwabara and T. Kanbara, *Macromol. Rapid Commun.*, 2013, **34**, 69; (h) D. H. Wang, A. Pron, M. Leclerc and A. J. Heeger, *Adv. Funct. Mater.*, 2013, **23**, 1297; (i) L. G. Mercier and M. Leclerc, *Acc. Chem. Res.*, 2013, **7**, 1597.
- 55 26 C. M. Cardona, W. Li, A. E. Kaifer, D. Stockdale and G. C. Bazan *Adv. Mater.* **2011**, **23**, 2367.
- 27 G. R. Fulmer, A. J. M. Miller, N. H. Sherden, H. E. Gottlieb, A. Nudelman, B. M. Stoltz, J. E. Bercaw and K. I. Goldberg, *Organometallics*, 2010, **29**, 2176.
- 28 I. Noviadri, K. N. Brown, D. S. Fleming, P. T. Gulyas, P. A. Lay, A. F. Masters and L. Phyllips, *J. Phys. Chem. B.*, 1999, **103**, 6713
- 29 P. Vanýsek, in *Handbook of Chemistry and Physics*, ed. D. R. Lide, CRC Press, Boca Raton, 89th edn., 2008–2009, p. 8-20.
- 65 30 Y. Nakajima, M. Hoshino, D. Yamashita and M. Uda, *Adv. Quantum Chem.*, 2003, **42**, 399
- 31 M. J. Frisch, G. W. Trucks, H. B. Schlogel, G. E. Scuseria, M. A. Robb, J. R. Cheeseman, G. Scalmani, V. Borone, B. Mennucci, G. A. Petersson, H. Nakatsuji, M. Caricato, X. Li, H. P. Hratchian, A. F. Izmaylov, J. Bloino, G. Zheng, J. L. Sonnenberg, M. Hada, M. Ehara,
- K. Toyota, R. Fukuda, J. Hasegawa, M. Ishida, T. Nakajima, Y. Honda, O. Kitao, H. Nakai, T. Vreven, J. A. Montgomery Jr., J. E. Peralta, F. Ogliaro, M. Bearpark, J. J. Heyd, E. Brothers, K. N. Kudin, V. N. Staroverov, R. Kobayashi, J. Normand, K. Raghavachari, A. Rendell, J. C. Burant, S. S. Iyengar, J. Tomasi, M. Cossi, N. Rega, J. M. Millam, M. Klene, J. E. Knox, J. B. Cross, V. Bakken, C. Adamo, J. Jaramillo, R. Gomperts, R. E. Stratmann, O. Yazyev, A. J. Austin, R. Cammi, C. Pomelli, J. W. Ochterski, R. L. Martin, K. Morokuma, V. G. Zakrzewski, G. A. Voth, P. Salvador, J. J. Dannenberg, S. Dapprich, A. D. Daniels, Ö. Farkas, J. B. Foresman, J. V. Ortiz, J. Cioslowski and D. J. Fox, Gaussian 09, Revision C.01, *Gaussian, Inc.*, Wallingford CT, 2009.
- 75 32 A. D. Becke, *J. Chem. Phys.*, 1993, **98**, 5648.
- 80 33 R. Dennington, T. Keith and J. Millam, GaussView, Version 5, *Semichem, Inc.*, Shawnee Mission KS, 2009.